

Two rotating particles interacting via two-body Gaussian potential harmonically confined in two spatial dimensions

Md Hamid^{1,*} and M.A.H. Ahsan¹

¹*Department of Physics, Jamia Millia Islamia
(Central University), New Delhi 110025, India.*

Abstract

We study two spinless bosons interacting via two-body Gaussian potential subjected to an externally impressed rotation about an axis confined in a harmonic trap in two-spatial dimensions. We obtain a transcendental equation for the relative angular momentum $|m|$ state with various values of the two-body interaction range σ and the two-body interaction strength g_2 to study the resulting energy spectrum and analyze the role of Hilbert space dimensions \tilde{N} . We compare results for both attractive and repulsive interaction for the δ -function potential and the Gaussian potential for various values of interaction range σ . We study the effects of interaction parameters and relative angular momentum on the ground state energy E_0 and its various components, namely, kinetic energy $\langle KE \rangle$, trap potential $\langle V \rangle$ and interaction potential $\langle PE \rangle$. For a given relative angular momentum $|m|$ and the non-interacting case, we observe that the ground state energy E_0 becomes independent of the interaction range σ . However, for a given relative angular momentum $|m|$ and the interaction strength $g_2 > 0$, there is an increase in the ground state energy E_0 with an increase in the interaction range σ . Below the interaction strength $g_2 V(r) \leq -1$, the ground state energy E_0 diverges to physically unacceptable negative-infinity for $|m| = 0$ state. Further, for $|m| = 1$, the ground state energy E_0 becomes independent of the interaction strength g_2 . For a relative angular momentum state $|m|$, we present a comparative study between the Gaussian interaction potential and the δ -function potential. Further, we observe that for a given g_2 and $|m|$, for δ -function potential *i.e.* $\sigma \rightarrow 0$, to achieve the convergence of ground state energy, we require a considerably large critical Hilbert space. Whereas, in the case of Gaussian interaction potential with $\sigma \rightarrow 1$, the ground state energy converges for a considerably small critical Hilbert space. We further observe that for the rotating case *i.e.* relative angular momentum $|m| \neq 0$, the interaction matrix elements become zero *i.e.* $I_{n'_r, n_r, |m|}(0) = 0$ and constant $I_{n'_r, n_r, 0}(0) = \alpha^2/\pi$ for $|m| = 0$,“ when $\sigma \rightarrow 0$.

* hamidjmi2008@gmail.com

I. INTRODUCTION

The problem of a single atom confined in a harmonic trap is one of the well-known quantum systems [1]. Going from a single atom to N confined atoms, physics becomes much involved. The recent development in last few decades in the technique of ultracold atomic cooling, trapping and manipulating of atoms [2] have opened up the possibility of studying the few bosons and fermions in a confined system in the lower dimensions [5, 18, 20].

The short-range inter-atomic interaction in quantum many-body systems like the dilute atomic vapours at low energies been analyzed theoretically in terms of the singular δ -function potential [9, 15, 21] with s -wave scattering length a_s . The sign of a_s is positive for repulsive interaction [7, 11, 26, 27] and negative for attractive interaction [16]. The present study of harmonically trapped two ultra-cold spinless bosons in quasi-2D plane, we employ Gaussian potential [5, 6, 22, 25] which unlike δ -interaction potential is smooth and provides control over inter-atomic interaction through the variation of two parameters, namely, the strength of interaction as measured by the s -wave scattering length a_s and the range of interaction as measured by the width of the Gaussian σ . To theoretically investigate the ground state properties of the two spinless bosons confined in a harmonic trap and interacting via a finite-range Gaussian potential in quasi-2D using exact diagonalization of the Hamiltonian. We study the ground state properties of the system by varying the interaction strength g_2 , the interaction range σ and the rotation parameter, relative angular momentum $|m|$.

We establish and discuss the connection between our finite-range treatment and contact δ -interaction results. The convergence of the ground state energy is faster in the finite-range interaction over the δ -interaction potential for given $|m|$. The role of the relative angular momentum $|m|$, has been significantly discussed in the present study to achieve the convergence of the system.

We organize this article as follows. In Sec. II, we derive the general Hamiltonian equation for two spinless bosons in quasi-2D symmetric plane. In Sec. IID, we derive the relation for the contact δ -interaction potential and study the leading spectrum and the size of active Hilbert space. In Sec. IIC, we establish a general relation for the finite-range potential to explore its effects on the two-body system in our study. In Sec. III we present our findings. Finally, in Sec. V we present a summary and conclusions. Supplement materials and numerics are deterred to the appendix.

II. THE SYSTEM AND THE HAMILTONIAN

In the present study of $N = 2$ spinless bosons each of mass M interacting via a normalized Gaussian potential in an x - y symmetric two-dimensional plane with an externally impressed rotation $\mathbf{\Omega} = \Omega \hat{z}$ about the z -axis. The Hamiltonian for the co-rotating system is given as:

$$\hat{\mathbf{H}}^{rot} = \hat{\mathbf{H}}^{lab} - \hat{\mathbf{\Omega}} \cdot \hat{\mathbf{L}}^{lab}$$

where $\hat{\mathbf{\Omega}} = \Omega \hat{e}_z$ is the angular velocity of the co-rotating frame and $\hat{\mathbf{L}}^{lab}$ is the total angular momentum of the system about the z -axis in the laboratory frame. Where the Hamiltonian in the laboratory frame is given as:

$$\begin{aligned} \hat{\mathbf{H}}^{lab} = & \sum_{i=1}^N \left[\frac{\hat{\mathbf{p}}_i^2}{2M} + V_{\text{trap}}(\mathbf{r}_{\perp i}) \right] + \frac{g_2}{2} \left(\frac{1}{\sqrt{2\pi}\sigma_{\perp}} \right)^2 \\ & \times \sum_{i \neq j} \exp \left[-\frac{(r_i - r_j)^2}{2\sigma^2} \right] \end{aligned} \quad (1)$$

and

$$\hat{\mathbf{L}}_z^{lab} = \sum_{i=1}^N \mathbf{r}_i \times \mathbf{p}_i = \sum_{i=1}^N \mathbf{I}_z^i.$$

The first term in the Hamiltonian Eq. (1) corresponds to the kinetic energy and the second term corresponds to the harmonic trap potential $V(\mathbf{r})$:

$$V_{\text{trap}}(\mathbf{r}) = \frac{1}{2} M \omega_{\perp}^2 r_{\perp}^2 \quad (2)$$

with $r_{\perp} = \sqrt{x^2 + y^2}$ is the normal radius from the axis of rotation and ω_{\perp} , ω_z are the radial and axial trap frequency of harmonic confinement respectively. In terms of these trapping frequencies, we can define harmonic oscillator lengths *i.e.* radial length $a_{\perp} = \sqrt{\frac{\hbar}{M\omega_{\perp}}}$ and axial trap length $a_z = \sqrt{\frac{\hbar}{M\omega_z}}$. The interaction strength in 3-D is given by ${}^3D g_2 = \frac{4\pi\hbar^2 a_s}{M}$ where a_s is the s-wave scattering length. The third term $V_{\text{int}}(\{\mathbf{r}, \mathbf{r}'\})$ is the inter-atomic Gaussian interaction potential discussed in the coming section.

A. The eigensolution in quasi-2D system

The total Hamiltonian of the system,

$$\hat{\mathbf{H}} = \hat{\mathbf{H}}_{\text{com}} + \hat{\mathbf{H}}_{\text{rel}} \quad (3)$$

can be separated in a non-interacting center of mass(COM) with total mass M and interacting relative(rel) coordinates with reduced mass $\mu = M/2$ in the following form.

$$\hat{\mathbf{H}}_{\text{com}} = -\frac{\hbar^2}{2M}\nabla_R^2 + \frac{1}{2}M\omega^2 R^2 \quad (4)$$

Hamiltonian eigenspectrum of COM is known, however the H_{rel} is to be calculated in co-rotating frame,

$$\begin{aligned} \hat{\mathbf{H}}_{\text{rel}} &= \sum_1^2 \left(\frac{-\hbar^2}{2\mu} \nabla_i^2 + \frac{1}{2}\mu\omega^2 \hat{\mathbf{r}}^2 \right) + g_2 V(\hat{\mathbf{r}}) - \hat{\mathbf{\Omega}} \cdot \hat{\mathbf{L}} \\ \hat{\mathbf{\Omega}} \cdot \hat{\mathbf{L}} &= \hat{\mathbf{\Omega}}(\hat{\mathbf{R}} \times \hat{\mathbf{P}} + \hat{\mathbf{r}} \times \hat{\mathbf{p}}) \end{aligned}$$

where the two-particles interaction finite-range Gaussian potential as,

$$V(\hat{\mathbf{r}}) = \left(\frac{1}{\sqrt{2\pi}\sigma} \right)^2 \sum_{i \neq j} \exp \left(-\frac{1}{2\sigma^2} (r_{\perp i} - r_{\perp j})^2 \right). \quad (5)$$

Here, ∇ is the 2-D Nabla operator, the problem is reduced in the center of mass $\mathbf{R} = \frac{1}{2}(\mathbf{r}_1 + \mathbf{r}_2)$ and relative coordinate system $\mathbf{r} = \mathbf{r}_1 - \mathbf{r}_2$

$$\hat{\mathbf{H}}_{\text{rel}} = \underbrace{-\frac{\hbar^2}{2\mu}\nabla_r^2 + \frac{1}{2}\mu\omega_{\perp}^2 \hat{\mathbf{r}}^2 - \hat{\mathbf{\Omega}} \cdot \hat{\mathbf{L}}}_{H_0} + g_2 V(\hat{\mathbf{r}}) \quad (6)$$

non-interacting COM motion is explicitly removed.

B. Solution for the interaction Hamiltonian

We start constructing the solution for the Hamiltonian in the relative coordinates system. A secular equation is established to study the quantities of interest in the following manner,

$$\hat{\mathbf{H}}_{\text{rel}} \Psi = \hat{\mathbf{E}} \Psi$$

where,

$$\Psi = \sum_{n_r, m}^{\infty} c_{n_r, m} u_{n_r, m} \quad (7)$$

Solution for relative Hamiltonian in Eq. (6) consists of Hamiltonian H_0 and the Gaussian interaction potential. The eigenstate Ψ can be expanded in the linear sum of single particle

basis state as $\Psi = \sum_{n_r, m}^{\infty} c_{n_r, m} |u_{n_r, m}\rangle$ with single particle relative angular momentum $|m|$ and radial quantum number n_r . For the Hamiltonian H_0 of the system, the eigenenergy is of the form of $\epsilon_{n_r, m} = (2n_r + 1 + |m| - m\Omega/\omega) \hbar\omega$ and eigenspectrum for the relative Hamiltonian in Eq.(6) is given below in Eq.(9) is known as the secular equation. The secular equation is being set up in the following manner, on $H_{\text{rel}}|\Psi\rangle = E|\Psi\rangle$, projecting $|u_{n_r', m'}\rangle$ from left, sets up the secular equation:

$$c_{n_r', m'}(\epsilon_{n_r', m'} - E) + g_2 \sum_{n_r=0, m}^{\infty} c_{n_r, m} \int_0^{\infty} \int_0^{2\pi} u_{n_r', m'}^*(r, \phi) V(r) u_{n_r, m}(r, \phi) r dr d\phi = 0 \quad (8)$$

writing Eq. (8) in the compact form as:

$$c_{n_r', m'}(\epsilon_{n_r', m'} - E) + g_2 \sum_{n_r=0, m}^{\infty} c_{n_r, m} I_{n_r', m'; n_r, m}(\sigma) = 0 \quad (9)$$

$$\text{where, } I_{n_r', m'; n_r, m}(\sigma) = u_{n_r', m'}^*(r, \phi) V(r) u_{n_r, m}(r, \phi) \quad (10)$$

The interaction matrix elements, $I_{n_r', n_r, |m|}(\sigma)$, is solved analytically in appendix A;

$$\begin{aligned} I_{n_r', n_r, |m|}(\sigma) &= \frac{(\alpha^2)^{1+|m|} (2\sigma^2)^{|m|}}{\pi (1 + 2\alpha^2 \sigma^2)^{n_r + n_r' + |m| + 1}} \\ &\times \sqrt{\frac{n_r!}{(n_r + |m|)!} \frac{n_r'!}{(n_r' + |m|)!}} \\ &\times \sum_{i=0}^{\min(n_r, n_r')} \binom{|m| + n_r}{|m| + i} \binom{|m| + n_r'}{|m| + i} \\ &\times \frac{(|m| + i)!}{i!} (2\alpha^2 \sigma^2)^{2i}, \end{aligned} \quad (11)$$

for zero-relative angular momentum $|m| = 0$, the Eq.(11) reduces to Eq. (7) of the reference [5],

$$\begin{aligned} I_{n_r', n_r, 0}(\sigma) &= \frac{\alpha^2}{\pi} \left(\frac{1}{1 + 2\alpha^2 \sigma^2} \right)^{n_r + n_r' + 1} \\ &\times {}_2F_1(-n_r', -n_r; 1, (2\alpha\sigma)^4) \end{aligned} \quad (12)$$

where,

$$\alpha = \sqrt{\frac{\mu\omega_{\perp}}{\hbar}} \text{ and } {}_2F_1 \text{ is Gauss-Hypergeometric function.}$$

C. Solution for Gaussian potential

To study the role of interaction range given by the width of a Gaussian potential, we first calculate the expansion coefficients $c_{n_r',m}$ using perturbation theory as in Appendix B.

$$c_{n_r,m} = -\frac{g_2 \langle u_{n_r,m} | W | u_{n_r',m} \rangle}{(\epsilon_{n_r,m} - E)} \quad (13)$$

substituting $n_{r'} = 0$ in Eq. (11) to get $I_{0,n_r,m}$ and hence the above expression becomes,

$$c_{n_r,m} = \frac{-g_2}{\epsilon_{n_r,m} - E} I_{0,n_r,m}(\sigma) C \quad (14)$$

substituting the above expression in Eq. (9)

$$\begin{aligned} & \frac{-g_2}{(\epsilon_{n_r',m} - E)} (\epsilon_{n_r',m} - E) I_{0,n_r,m}(\sigma) C \\ & + g_2 \sum_{n_r}^{\infty} \frac{-g_2}{\epsilon_{n_r,m} - E} I_{0,n_r,m}(\sigma) C I_{n_r',n_r,m}(\sigma) = 0 \end{aligned}$$

which on simplification, takes the following form

$$\begin{aligned} I_{0,n_r',m}(\sigma) + g_2 \sum_{n_r}^{\infty} \frac{1}{\epsilon_{n_r,m} - E} I_{0,n_r,m}(\sigma) \\ \times I_{n_r',n_r,m}(\sigma) = 0 \end{aligned} \quad (15)$$

substituting $n_{r'} = 0$, the above Equation becomes

$$I_{0,0,m}(\sigma) + g_2 \sum_{n_r}^{\infty} \frac{1}{\epsilon_{n_r,m} - E} I_{0,n_r,m}^2(\sigma) = 0 \quad (16)$$

substituting the following two Eqs. (17) and (18) obtained from the Eq. (11) into above Eq. (16), simplify to the final expression Eq. (19) of this article.

$$I_{0,0,m}(\sigma) = \frac{(\alpha^2)^{1+|m|} (2\sigma^2)^{|m|}}{\pi(1 + 2\alpha^2\sigma^2)^{1+|m|}} \quad (17)$$

and

$$\begin{aligned} I_{0,n_r,m}(\sigma) &= \sqrt{\frac{n_r!}{(n_r + |m|)! (|m|)!}} \\ &\times \frac{(\alpha^2)^{1+|m|} (2\sigma^2)^{|m|}}{\pi(1 + 2\alpha^2\sigma^2)^{1+n_r+|m|}} \frac{(|m| + n_r)!}{n_r!} \end{aligned} \quad (18)$$

thus final expression becomes,

$$\begin{aligned}
& \frac{\pi (|m|!)^2}{(2\sigma^2)^{|m|}(\alpha^2)^{1+|m|}} (1 + 2\alpha^2\sigma^2)^{1+|m|} \\
& + \frac{g_2}{\hbar\omega_\perp} \times \sum_{n_r=0}^{\infty} \frac{1}{2n_r + 1 + |m| - E/\hbar\omega_\perp - m\hbar\Omega/\omega_\perp} \\
& \times \left(\frac{1}{1 + 2\alpha^2\sigma^2} \right)^{2n_r} \frac{(|m| + n_r)!}{n_r!} = 0
\end{aligned} \tag{19}$$

The above analytical solution for the generalized angular momentum $|m|$ in Eq. (19) is the main analytical result of this article. We can study the system for general relative angular momentum $|m| = 0, \pm 1, \pm 2 \dots$. For study purposes, we choose only two values i.e. 0 (even-parity satisfied by bosons) and 1 (odd-parity satisfied by fermions). For $|m| = 0$, the above Eq. (19) reduces to the following equation which reduces to Eq.(17) of reference [5].

$$\frac{\hbar\omega_\perp}{g_2} = -\frac{\alpha^2}{2\pi(1 + 2\alpha^2\sigma^2)} \Phi \left[\frac{1}{(1 + 2\sigma^2\alpha^2)^2}, 1, \frac{1 - E/\hbar\omega_\perp}{2} \right] \tag{20}$$

where, Φ is Lerch transcendent function.

Eq. (19) is the main analytical relation calculated for the general angular momentum of interacting Hamiltonian. This is used to calculate the energy-spectrum for the N= 2-spin-0 particle interacting via a finite range Gaussian potential in quasi 2-D plane for the given parameters $g_2, |m|, \sigma$ and α , etc. Numerical results are presented in the coming sections.

D. Solution for $\sigma \rightarrow 0$ in relative angular momentum $|m|$

The results in above section reduces to the contact δ -function potential. Following Eq. (11), for the rotating case of non-zero relative angular momentum ($|m| \neq 0$), the interaction matrix elements become $I_{n'_r, n_r, |m|}(0) = 0$, i.e. the interaction Hamiltonian becomes zero for δ -function and for non-rotating case ($|m| = 0$) the interaction matrix elements $I_{n'_r, n_r, 0}(0) = \alpha^2/\pi$, becomes a constant, this will leads the way to study the finite range effects on the system, thus the Eq. (9) becomes similar as in article[5],

$$c_{n'_r, 0}(\epsilon_{n'_r, 0} - E) + g_2 \sum_{n_r=0}^{\infty} c_{n_r, 0} \frac{\alpha^2}{\pi} = 0 \tag{21}$$

using the variational calculation, we can find the form of $c_{n'_r, 0} = -\frac{g_2 C}{\epsilon_{n'_r, 0} - E}$, where C is again a constant, rearranging the above Eq. (21), we get the energy relation. Truncating the

summation to a finite size of Hilbert space \tilde{N} , and studying the energy spectrum.

$$\frac{\pi}{\alpha^2} + g_2 \sum_{n_r=0}^{\tilde{N}_c} \frac{1}{\epsilon_{n_r,0} - E} = 0 \quad (22)$$

writing $\epsilon_{n_r,0} = (2n_r + 1)\hbar\omega$ and making the above equation dimensionless.

$$\frac{\pi}{\alpha^2} + \frac{g_2}{\hbar\omega_\perp} \sum_{n_r=0}^{\tilde{N}_c} \frac{1}{2n_r + 1 - E/\hbar\omega_\perp} = 0 \quad (23)$$

from the above equation, setting $\alpha = 1$, we can get the information about the energy spectrum of our system as a function of Hilbert space \tilde{N} . The above series is a harmonic series and divergent[24]. To obtain a meaningful sum we first terminate the sum at finite \tilde{N} and then truncate the sum at $\tilde{N} \rightarrow \infty$ to study the large range order. These Figs. 1-6 has been discussed to present the study of the ground state energy E_0 vs \tilde{N} for different interaction parameters.

III. NUMERICAL RESULTS AND DISCUSSION

For ^{87}Rb atom, the size of system turns out to be $a_\perp = \sqrt{\frac{\hbar}{M\omega_\perp}} = 733$ nm with $\omega_\perp = 2\pi \times 220$ Hz. The dimensionless interaction strength parameter g_2 , is taken in the range -4 to $+4$ in the present study. The Gaussian-shaped two-body potential allows us to tune the interaction parameter σ . The energy spectrum for different values of the interaction range σ and the interaction strength g_2 (attractive and repulsive) is being examined to study the size of Hilbert space or basis states for given relative angular momentum $|m|$. Various components of the energy spectrum namely the interaction energy $\langle V \rangle$, the kinetic energy $\langle KE \rangle$ and the potential energy $\langle PE \rangle$ is also computed and our scheme establish this relationship $\langle E \rangle = \langle V \rangle + \langle KE \rangle + \langle PE \rangle$. Here we present the results from Eq. (19) to study the energy spectrum of the system under study for different parameters to lay down an analytical ground and establish the computational rationale.

In Fig. 1, we present the ground state energy E_0 vs size of the Hilbert space \tilde{N} for the pair in relative coordinates. For zero relative angular momentum $|m| = 0$ and both type of interaction strength g_2 i.e. $g_2 > 0$ and < 0 . For the positive interaction strength $g_2 = +1, +2, +3$ and $+4$, we observe an upward shift in the ground state energy with increasing interaction strength g_2 . The higher the interaction strength, the higher the ground

state energy. For a given value of g_2 , there is a critical size of the Hilbert space $\tilde{N}_c(g_2)$ beyond which the ground state energy saturates and becomes independent of the size of the Hilbert space $\tilde{N}(g_2)$. The critical size of Hilbert space is a point beyond which the ground state energy E_0 gets saturated for a given set of parameters. For example, for $g_2 = +1$, the saturated ground state energy is 1.206 at the critical size of Hilbert space $\tilde{N}_c = 33$ and for $g_2 = +4$, the saturated ground state energy (E_{sat}) is 1.396 at the critical size of Hilbert space $\tilde{N}_c = 52$. For attractive interaction strength $g_2 = -1$, we observe that the ground state energy diverges from the zero-point energy and becomes saturated at $E_{sat} = 0.425$ for the critical size of Hilbert space $\tilde{N}_c = 81$. Below $g_2 < -1$, the system becomes a lump and hence not being subjected to any statistical laws hence there is no need to go beyond it. We observe that with increase in g_2 , the ground state energy shifts away from zero-point energy, $E_0(E_{sat}, g_2, N_c) = E_0(1.19, +1, 32)$ and $E_0(1.396, +4, 52)$. The ground state energy E_0 diverges from zero-point energy for negative interaction strength.

To further study the system, we present the study of ground state energy E_0 vs size of the Hilbert space \tilde{N} for relative angular momentum $|m| = 1$ (rotating) in Fig. 2. For positive interaction strength $g_2 = +1, +2, +3, +4$, we observe that the ground state energy E_0 , increases with increasing interaction strength. For example, for $g_2 = +4$, the saturated ground state energy $E_0(E_{sat}, g_2, \tilde{N}_c) = E_0(2.018, +4, 47)$ and for $g_2 = +1$ is $E_0(2.005, +1, 6)$, hence with increasing g_2 pair requires large Hilbert space to achieve saturation. For negative interaction strength $g_2 = -1, -2, -3, -4$, the ground state energy decreases with decreasing interaction strength g_2 . The critical size of Hilbert space \tilde{N}_c increases with decrease in the interaction strength g_2 , for example $E_0(1.993, -1, 4)$, $E_0(1.975, -3, 72)$ and $E_0(1.961, -4, 136)$. In comparison to Fig. 1, we observed that the saturation in the ground state energy has an upward shift with increase in relative angular momentum $|m|$, from 0 to 1, for fixed interaction range σ , which is expected from the eigenenergy relation $\epsilon_{n_r, |m|} = 2(n_r + |m| + 1)\hbar\omega$.

In Fig. 3, we present the study of ground state energy E_0 vs size of the Hilbert space \tilde{N} for relative angular momentum $|m| = 0$ (non-rotating) and positive interaction strength $g_2 = +1$ for different values of interaction range σ . Here, we observe that the ground state energy shifts toward the zero-point energy with the increase in interaction range σ . Further, we observe that for zero-contact δ -interaction ($\sigma = 0.001 \equiv 0$), the slope of ground state energy E_0 shows a divergent trend, it attains the non-interacting energy for large \tilde{N} . Our observation suggests that as the interaction range σ increases, the size of the criti-

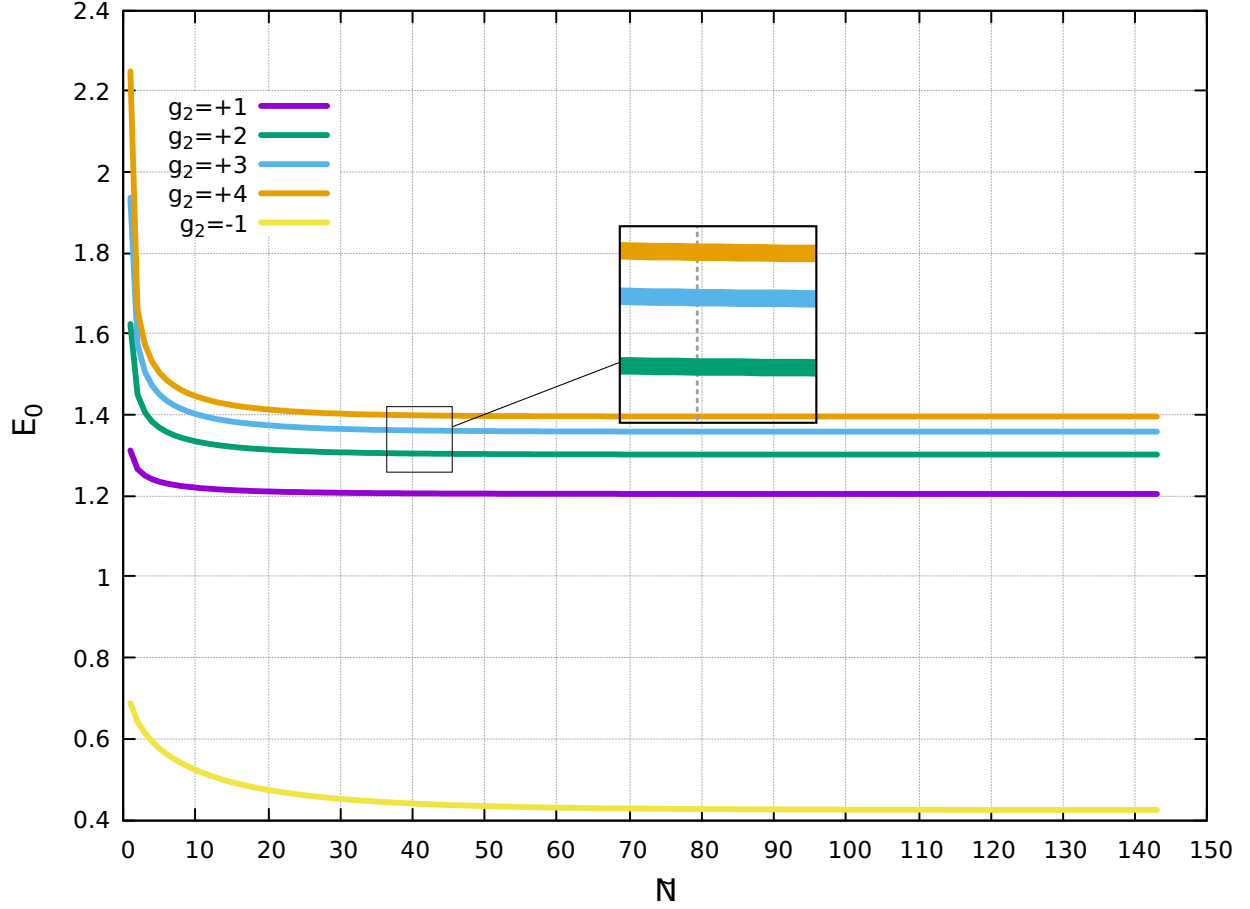


FIG. 1: (Colour online) Ground state energy (E_0) in relative co-ordinative angular momentum $|m| = 0$. The quantities E_0 and g_2 are being measured in units of $\hbar\omega$ and \hbar^2/m respectively. Inset shows magnified views of some energy spectrum.

cal Hilbert space decreases, here are some results in terms of increasing interaction range, $E_0(E_{sat}, \sigma, \tilde{N}_c) = E_0(1.226, 0.2, 14)$, $E_0(1.228, 0.3, 7)$ and $E_0(1.199, 0.5, 6)$. It has been observed that the ground state energy gets well saturated in the case of a higher interaction range i.e. $\sigma = 0.3$ to 0.9 in contrast to the lower interaction range, say $\sigma = 0.001$ to 0.2 . Thus our observation that the use of finite range potential is the best suit for the over zero-contact δ -function is verified.

In Fig. 4, to further study the system for relative angular momentum $|m| = 1$ (rotating), we present the study of ground state energy E_0 vs size of the Hilbert space \tilde{N} for a fixed value of interaction strength $g_2 = +1$ and different interaction range σ . We observe an upward shift in the E_0 with an increase in the σ . For the interaction range $\sigma = 0.0001$ and

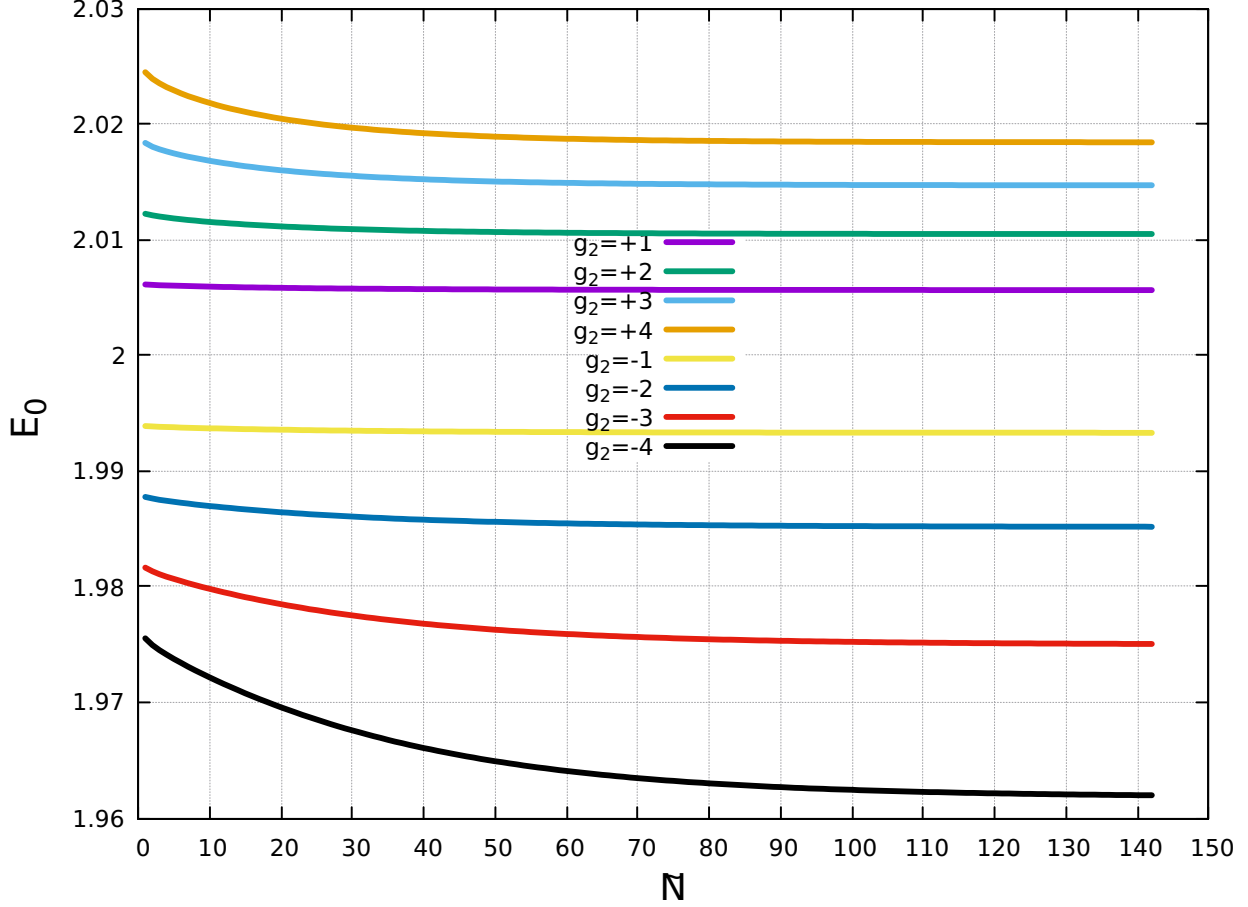


FIG. 2: (Colour online) Ground state energy E_0 in relative co-ordinate vs size of the Hilbert space (\tilde{N}) for different values of interaction strength g_2 and fixed value of interaction range $\sigma = 0.1$ with relative angular momentum $|m| = 1$. The quantities E_0 and g_2 are being measured in units of $\hbar\omega$ and \hbar^2/m respectively.

0.1, the ground state energy is saturated for a small value of \tilde{N}_c . We also observe that for the interaction range $\sigma = 0.2$ and beyond, E_0 first decreases and then becomes constant. We observe that ground state energy does not feel interaction for $|m| = 1$ (odd parity) and becomes independent of the size of the Hilbert space around $\tilde{N} = 20$.

In Fig. 5, we present the study of ground state energy E_0 vs size of the Hilbert space \tilde{N} , for negative interaction strength $g_2 = -1$ with relative angular momentum $|m| = 0$ (non-rotating). We observe that the E_0 shifts toward zero-point energy with increasing σ . For $\sigma = 0.001$ ($\sigma \rightarrow 0$), the nature of slope for E_0 is divergent and saturation is asymptotic in nature. For example, $E_0(E_{sat}, \sigma, \tilde{N}_c) = E_0(0.42, 0.1, 73)$ and $E_0(0.77, 0.5, 6)$, we con-

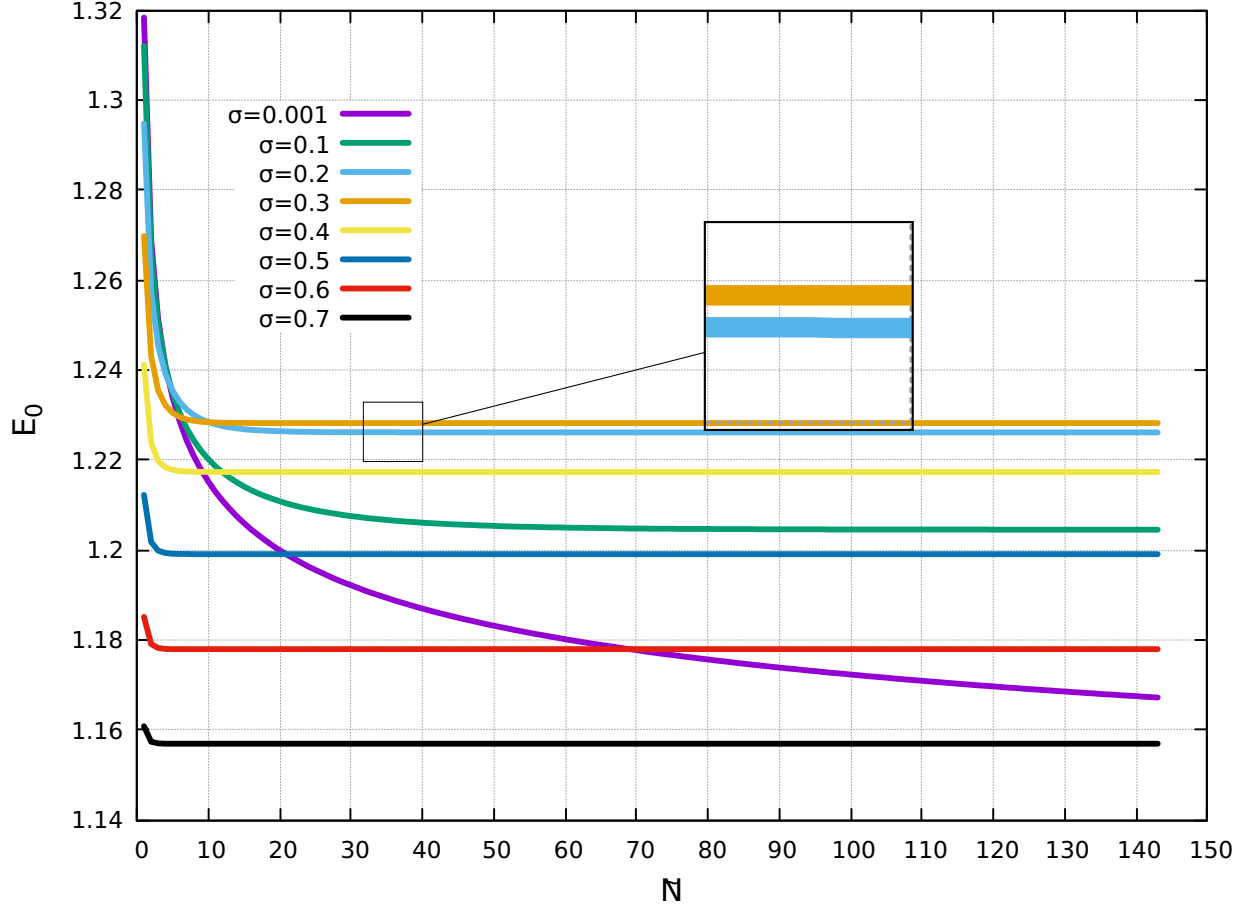


FIG. 3: (Colour online) Ground state energy E_0 in the relative co-ordinate *vs* size of the Hilbert space \tilde{N} for different values of interaction range σ and a fixed value of interaction strength $g_2 = +1$, for relative angular momentum $|m| = 0$. The quantities E_0 and σ are being measured in units of $\hbar\omega$ and $\sqrt{\frac{\hbar}{m\omega}}$ respectively. In the inset, we magnify the energy spectrum.

clude that the size of critical Hilbert space \tilde{N}_c decreases with increase in σ . In the case of $\sigma = 0.4, 0.5, 0.7$ and $= 0.9$, the deviation in E_0 is constant.

In this Fig. 6, we present the study of ground energy E_0 *vs* size of the Hilbert space \tilde{N} for a fixed interaction strength parameter $g_2 = -1$ with relative angular momentum $|m| = 1$ (rotating) for different interaction range σ . We observe that there is the decrease in energy E_0 with increasing interaction range σ . Ground state energy E_0 in terms of σ is $E_0(1.976, 0.2, 6)$ $E_0(1.956, 0.3, 3)$. The ground state energy E_0 does not depend much on σ in rotating angular momentum $|m| = 1$.

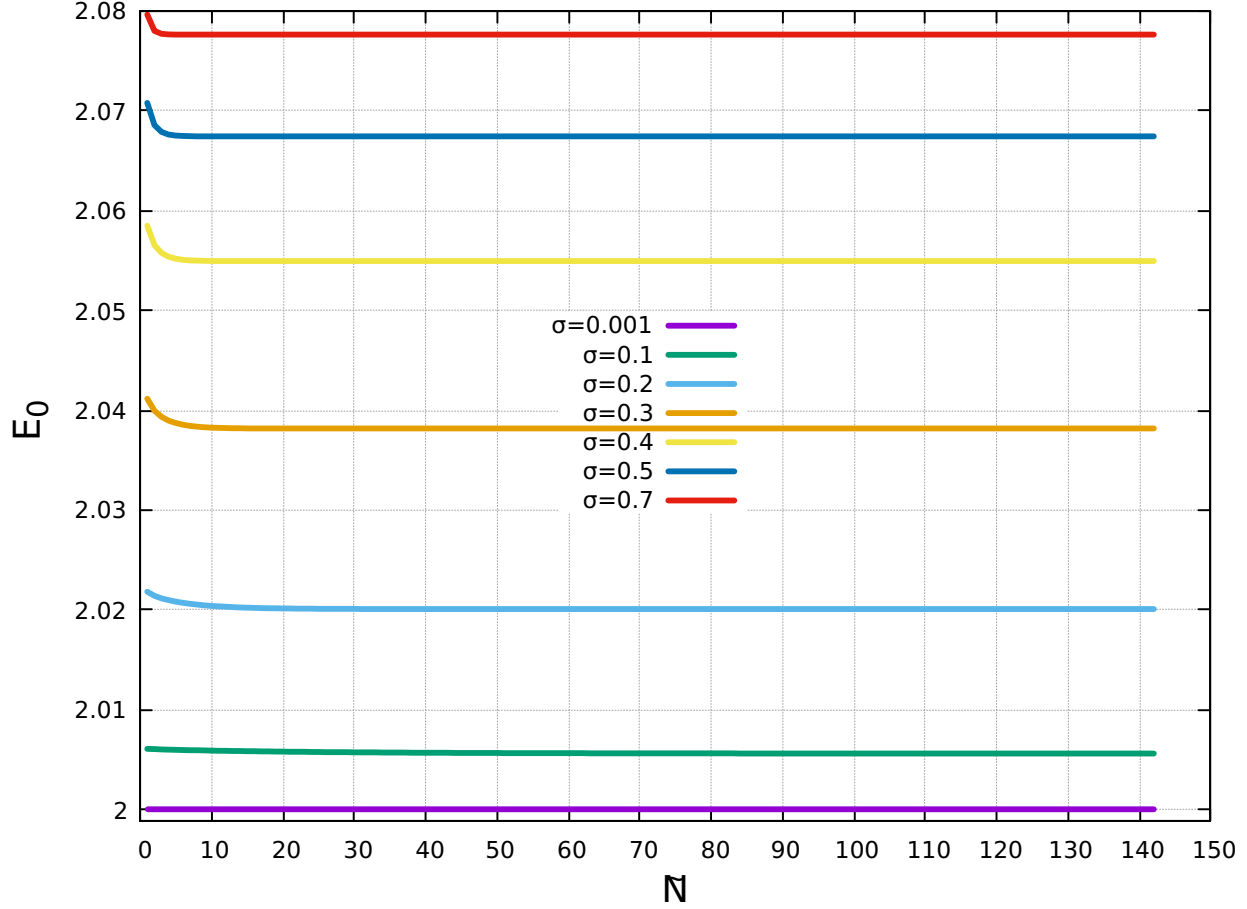


FIG. 4: (Colour online) Ground state energy E_0 in the relative co-ordinate vs size of the Hilbert space \tilde{N} for different values of interaction range σ and a fixed value of interaction strength $g_2 = +1$, for relative angular momentum $|m| = 1$. The quantities E_0 and σ are being measured in units of $\hbar\omega$ and $\sqrt{\frac{\hbar}{m\omega}}$ respectively.

In the Fig. 7, we present the study of energy spectrum E , in relative coordinates vs the interaction strength g_2 with the relative angular momentum $|m| = 0$ and 1. The first three energy in relative angular momentum $|m| = 0$, such as $(E_0, |m| = 0)$, $(E_1, |m| = 0)$ and $(E_2, |m| = 0)$ corresponds to ground, first and the second excited energy respectively. For relative angular momentum $|m| = 1$ the energy, $(E_0, |m| = 1)$, $(E_1, |m| = 1)$ and $(E_2, |m| = 1)$ correspond to ground, first and second excited state energy respectively. The energy spectrum in the case of relative angular momentum $|m| = 1$ shows no dependence on the interaction strength parameter g_2 in both regions. In other words for odd parity $|m| = 1$ (rotating), particles do not experience interaction in either region of strength g_2 .

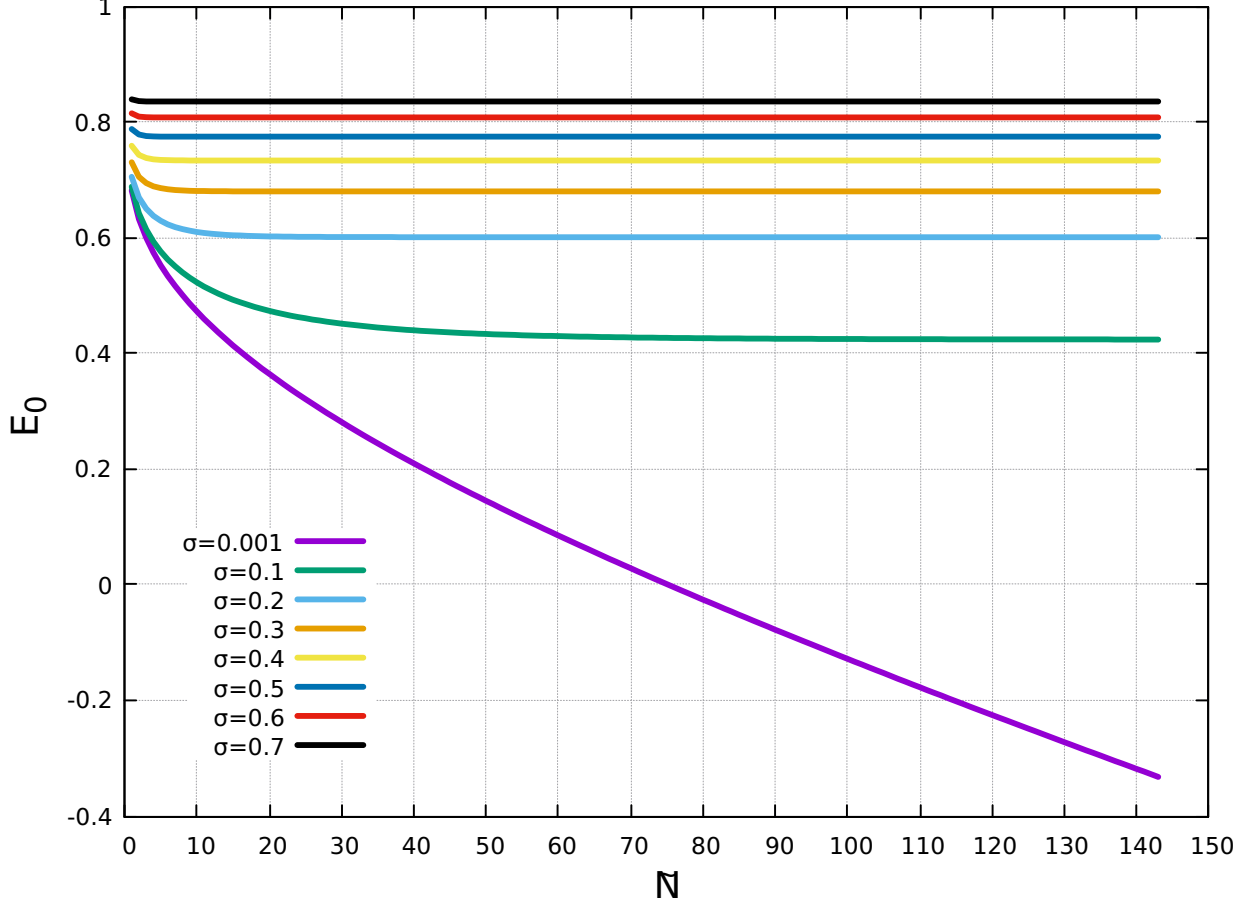


FIG. 5: (Colour online) The ground state energy E_0 in relative co-ordinate *vs* size of Hilbert space \tilde{N} for the different values of interaction range σ , fixed attractive interaction strength $g_2 = -1$ and zero relative angular momentum ($|m| = 0$). The quantities E_0 and σ are being measured in units of $\hbar\omega$ and $\sqrt{\frac{\hbar}{m\omega}}$ respectively.

Non-rotating ground state energy E_0 , for relative angular momentum $|m| = 0$, in the attractive interaction range $g_2 < 0$, becomes negative and even diverged to $-\infty$, making the system an un-physical one, that is why we argued that the system is no more physical beyond the interaction strength $g \leq -1$ and for $g_2 \geq 0$ the system tends to acquire the non-interacting state over the range. At zero interaction strength, the energy difference between the consecutive energy levels i.e. $E_1 - E_0 = E_2 - E_1 = 2\hbar\omega_\perp$ i.e. breathing energy[25] for both zero and non-zero relative angular momentum $|m|$, further, we recover the non-interacting energy $E(n_r, |m|) = (2n_r + |m| + 1)\hbar\omega$.

In Fig. 8, we plot the average trap potential $\langle V \rangle$ *vs* interaction strength g_2 for relative

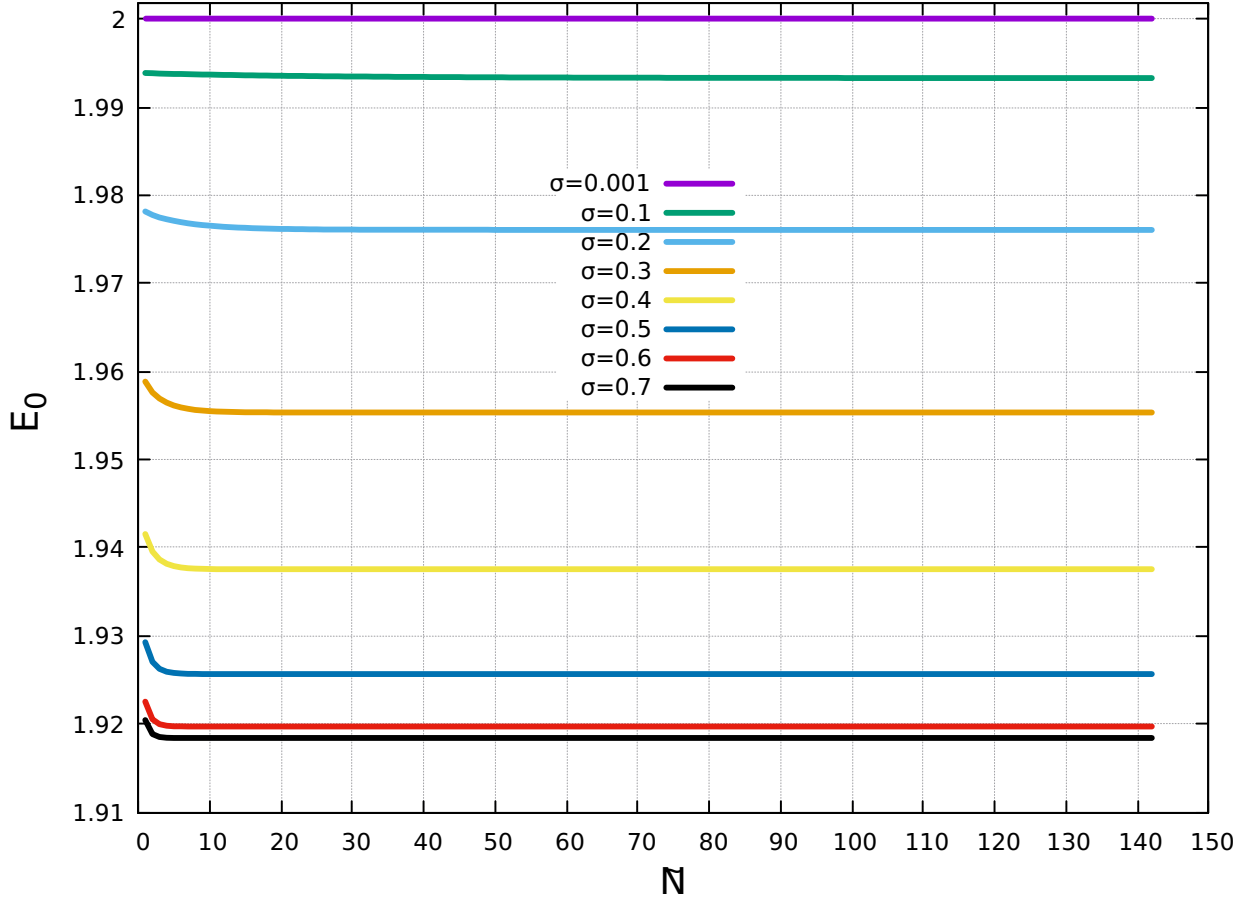


FIG. 6: (Colour online) Ground state energy E_0 in the relative co-ordinates *vs* size of the Hilbert space \tilde{N} for different values of interaction range σ and fixed value of interaction strength $g_2 = -1$, for relative angular momentum $|m| = 1$. The quantities E_0 and σ are being measured in units of $\hbar\omega$ and $\sqrt{\frac{\hbar}{m\omega}}$ respectively.

angular momentum $|m| = 1$ and interaction range $\sigma = 0.1$. The $\langle V_0 \rangle$, $\langle V_1 \rangle$ and $\langle V_2 \rangle$ are the ground, first and the second excited state energy respectively. We have observed that the average trap potential energy increases with the increasing interaction strength. We also observe that at $g_2 = 0$, contribution is zero, means $E_0 = \langle KE \rangle + \langle H_{\text{int}} \rangle$ only has non-zero contribution.

In Fig. 9, we plot ground state energy E_0 , average interaction, kinetic and potential energy *vs* interaction range σ , for interaction strength $g_2 = +1$ and relative angular momentum $m = 0$. For E_0 , we have observed that the ground state energy, first increases and attains a peak at $\sigma = 0.4$ and then starts decreasing with increasing σ . $\langle V \rangle$ and

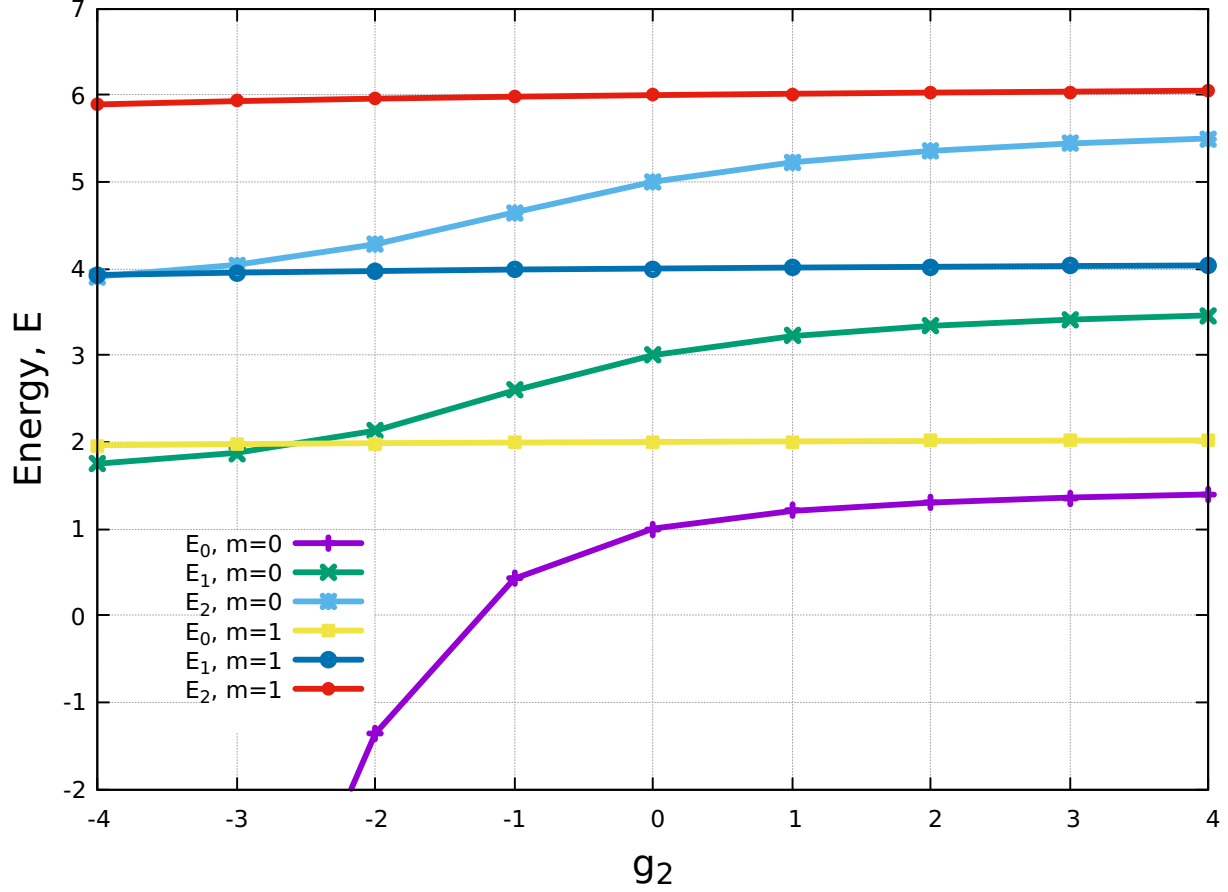


FIG. 7: (Colour online) Energy E in relative co-ordinate *vs* interaction strength g_2 , for relative angular momentum $|m| = 0$, and 1, the interaction range $\sigma = 0.1$ is plotted to study the energy-spectrum. Energy and g_2 are units of $\hbar\omega$ and \hbar^2/m respectively.

$\langle PE \rangle$ follow the same trend as of E_0 on contrast the $\langle KE \rangle$, first decreases attains a minimum at $\sigma = 0.4$ and then increases with system size. Sum of all three energies, i.e. $\langle V \rangle + \langle KE \rangle + \langle PE \rangle = E_0$ for all σ .

In Fig. 10, we plot ground state E_0 , average interaction $\langle V \rangle$, kinetic energy $\langle KE \rangle$ and potential energy $\langle PE \rangle$ *vs* interaction range σ for interaction strength $g_2 = -1$ and relative angular momentum $|m| = 1$ (rotating). We observe that $E_0, \langle V \rangle$ and $\langle PE \rangle$ have been continuously increasing with system size in contrast with $\langle KE \rangle$, which is continuously decreasing. Sum of all three energies, i.e. $\langle V \rangle + \langle KE \rangle + \langle PE \rangle = E_0$ for all σ .

In the Fig. 11, we study the ground state energy E_0 *vs* the interaction strength parameter

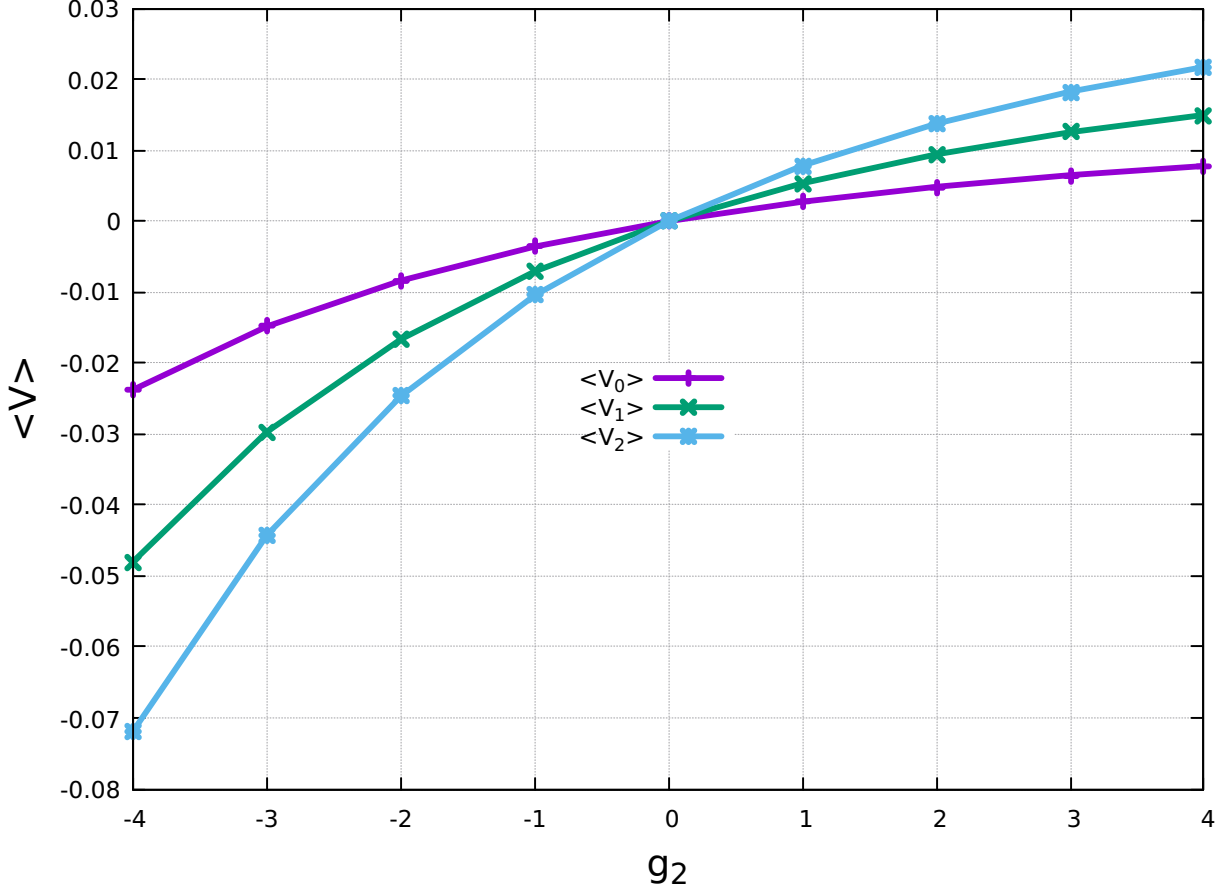


FIG. 8: (Colour online) The average interaction energy $\langle V \rangle$ against interaction strength g_2 , relative angular momentum ($|m| = 1$) for the fixed interaction range σ is plotted to study the energy spectrum. The quantities $\langle V_0 \rangle$, $\langle V_1 \rangle$, $\langle V_2 \rangle$ are being measured in units of $\hbar\omega$ and σ is being measured in $\sqrt{\frac{\hbar}{m\omega}}$ respectively.

g_2 for relative angular momentum $|m| = 0, 1$ and the ratio of frequencies $\Omega/\omega = 0.1$ for the different values of interaction range σ . For relative angular momentum $|m| = 0$, the energy spectrum is slightly increasing with decreasing slope while for the relative angular momentum $|m| = 1$ has constant growth with constant slope. The energy increases with the increase in interaction range. There is an upward shift in energy with the increase in the relative angular momentum $|m|$ from 0 to 1. There is an increase in the energy gap with an increase in interaction strength.

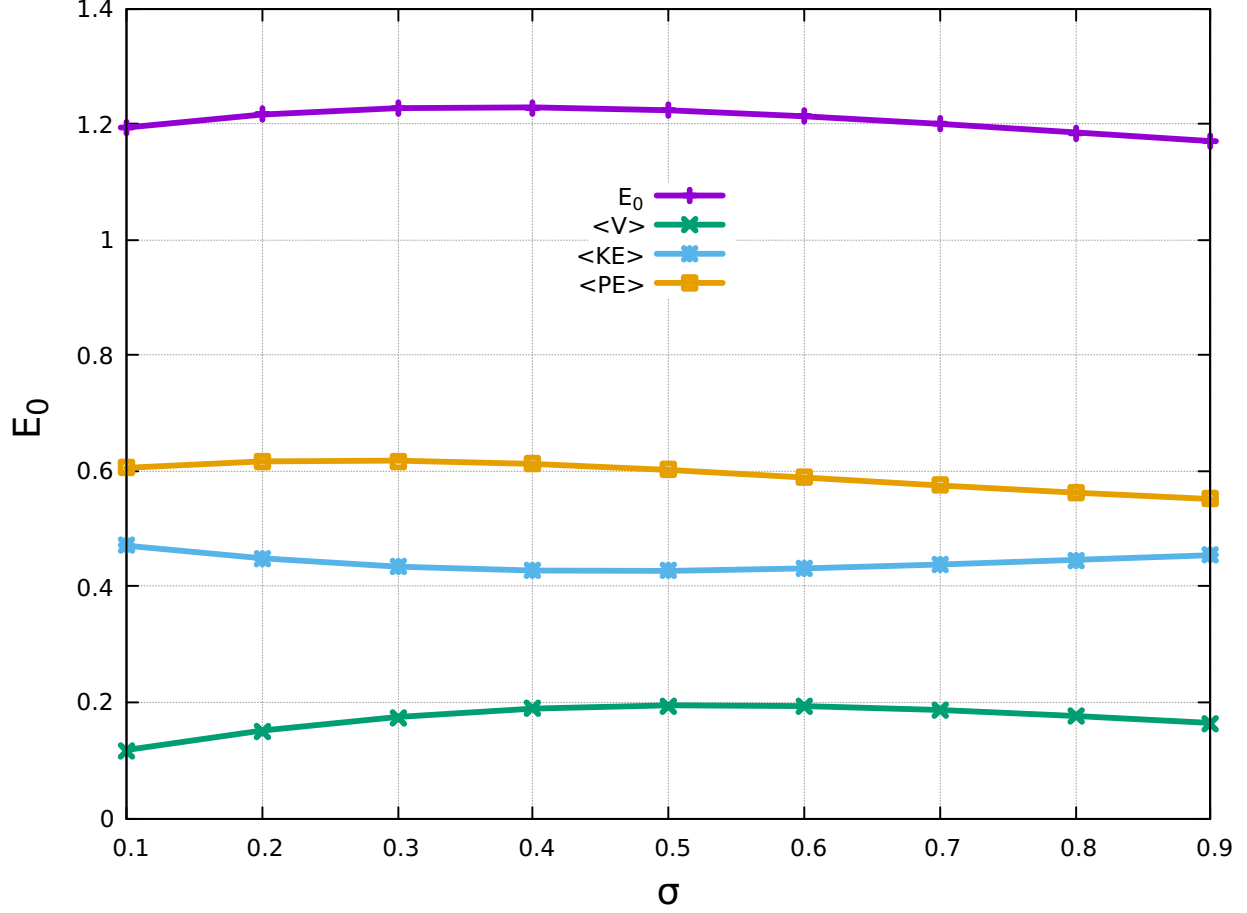


FIG. 9: (Colour online) Ground state energy E_0 , average interaction, kinetic and potential and trap potential energy *vs* interaction range σ for relative angular momentum $|m| = 0$ and interaction strength $g_2 = +1$ is plotted to study the energy spectrum. The quantities $E_0, \langle V \rangle, \langle KE \rangle, \langle PE \rangle$ are being measured in units of $\hbar\omega$ and σ in $\sqrt{\frac{\hbar}{m\omega}}$ respectively.

IV. CONDITIONAL PROBABILITY DENSITY

To further probe the particle density co-relation, Conditional Probability Density (CPD) is being calculated. The CPD is the measure of an intrinsic density distribution of bosons which makes it an experimental observable quantity over the circularly(cylindrical) symmetric density distribution. The CPDs $\rho(\mathbf{r}, \mathbf{r}_0)$ is defined as the probability of finding one particle at position \mathbf{r} given that the other particle is at \mathbf{r}_0 is mathematically defined as. [28] The probability of finding a particle at position \mathbf{r} given that the other particle is at \mathbf{r}_0 . The

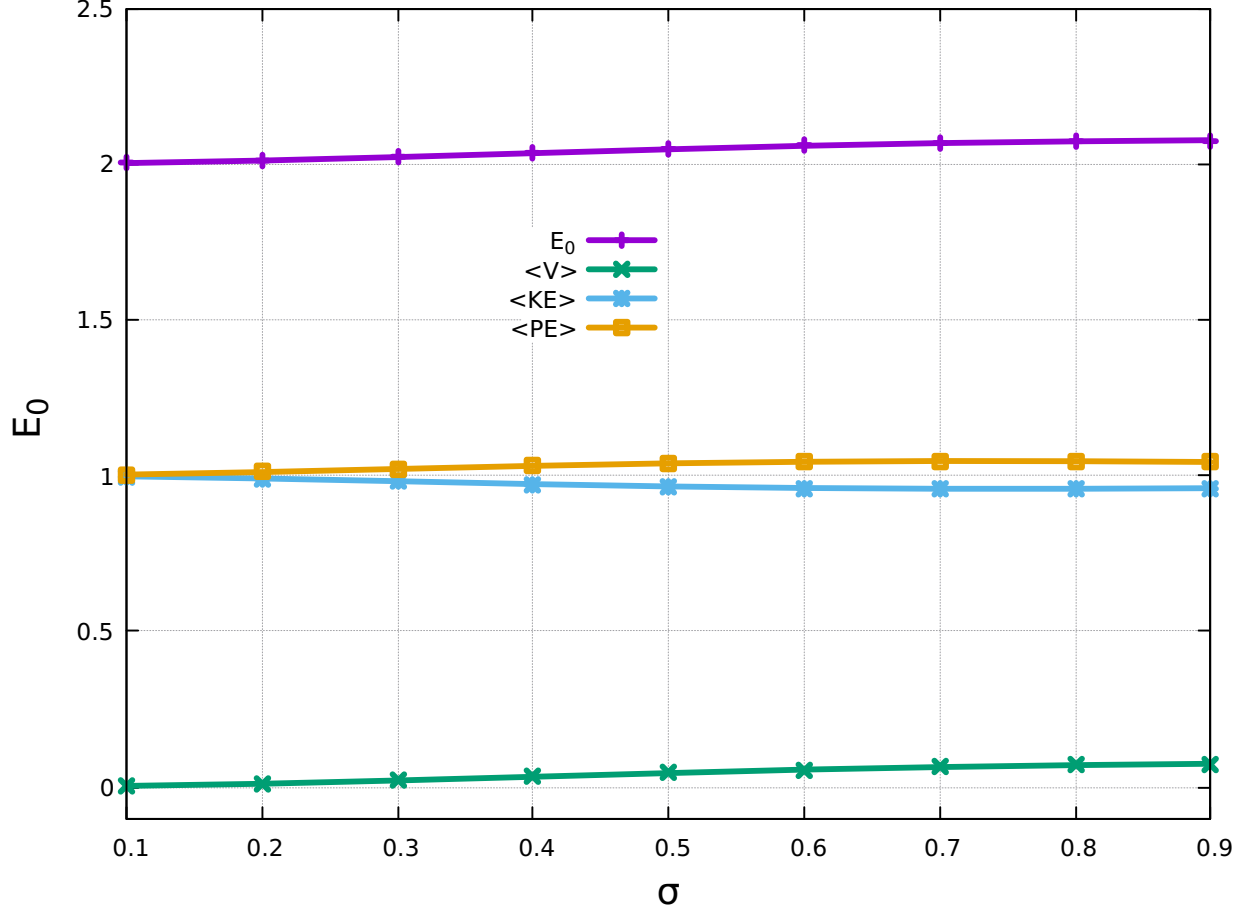


FIG. 10: (Colour online) Ground state energy E_0 , average interaction, kinetic and trap potential energy *vs* interaction range σ for relative angular momentum $|m| = 1$ and interaction strength $g_2 = +1$ is plotted to study the spectrum of energy. The quantities $E_0, \langle V \rangle, \langle KE \rangle, \langle PE \rangle$ are being measured in units of $\hbar\omega$ and σ in $\sqrt{\frac{\hbar}{m\omega}}$ respectively.

mathematical expression is as follows,

$$\rho(\mathbf{r}, \mathbf{r}_0) = \frac{\sum_{i \neq j} \langle \Psi | \delta(\mathbf{r} - \mathbf{r}_i) \delta(\mathbf{r}_0 - \mathbf{r}_j) | \Psi \rangle}{(N-1) \sum_j \langle \Psi | \delta(\mathbf{r}_0 - \mathbf{r}_j) | \Psi \rangle}$$

Where $\langle \Psi |$ is the many-body eigensolution obtained by exact diagonalization and \mathbf{r}_0 is the reference points can be chosen at $(x = 0, y = 0)$ or any points where the density is to observe. Fig. 12, we observe the Gaussian symmetry for different interaction strength g_2 and total angular momentum L_z state.

In the Table I, we summarise the size of critical Hilbert space \tilde{N}_c and saturated ground

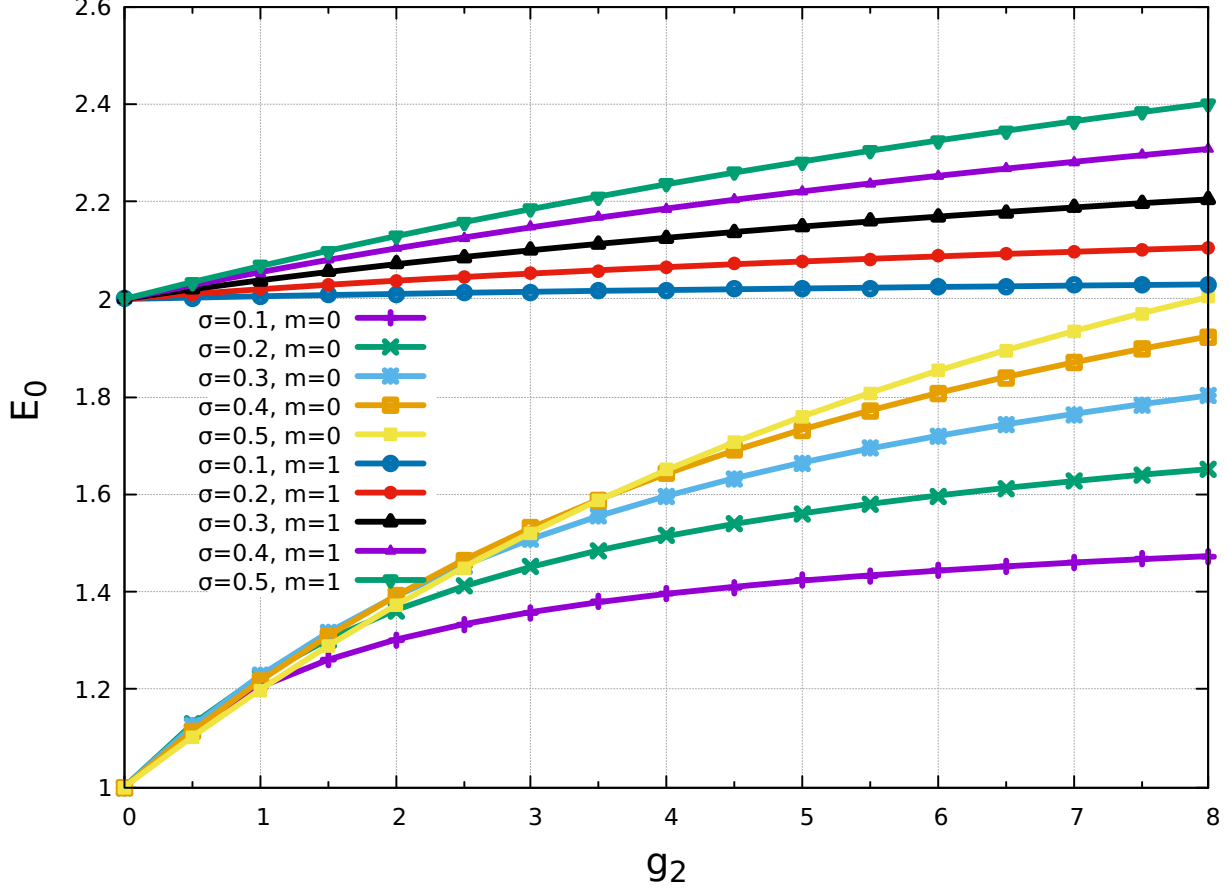


FIG. 11: (Color online) Ground state energy E_0 in rotating $|m| = 1$ and non-rotating $|m| = 0$ as a function of interaction g_2 and for the range $\sigma = 0.1, 0.2, 0.3, 0.4$ and 0.5 is plotted to study the energy spectrum. The quantities E_0 and g_2 are being measured in units of $\hbar\omega$.

state energy E_0 against the interaction range $0.1 \leq \sigma \leq 0.9$. We observe that as the interaction range increases the size of Hilbert space decreases for the interaction strength $g_2 = \pm 1$. In Table. II, We observe the size of critical Hilbert space \tilde{N}_c and saturated ground state energy E_{sat} against the interaction strength $-4 \leq g_2 \leq +4$ for a given interaction range $\sigma = 0.10$ and single particles angular momentum $|m| = 0, 1$.

V. SUMMARY AND CONCLUSION

We derive the general relation for angular momentum $|m|$ of the interacting Hamiltonian and analyze the ground state energy-spectrum in its subspace. We explore the contact δ -

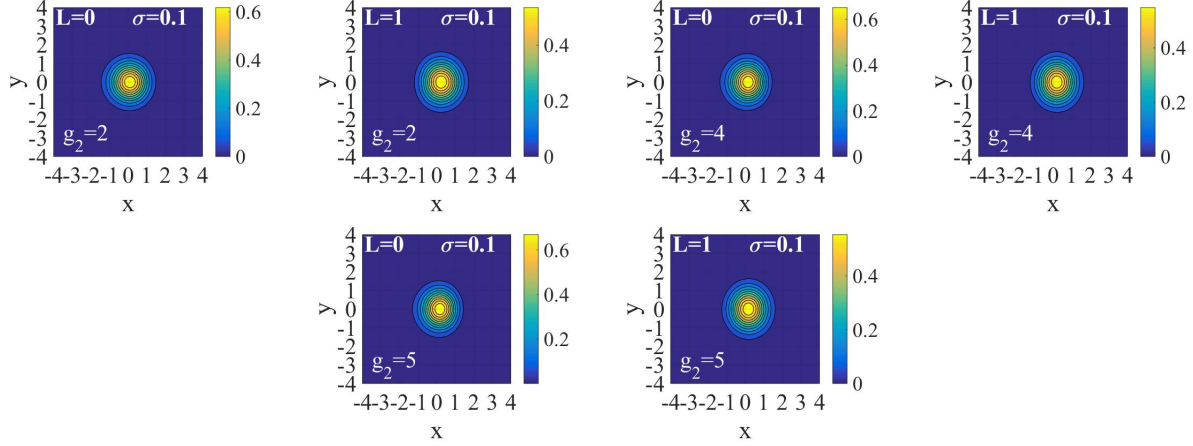


FIG. 12: (Color online)CPDs contour plots for $N=2$ spin-0 bosons in subspace of total angular momentum L_z with interaction strength g_2 and interaction range σ in the finite range smooth Gaussian potential in Eq. (1). These contour plots are iso-surface density profiles viewed along the rotation axis- z . The reference point is chosen relatively large $\mathbf{r}_0 = (x_0, y_0) = (3, 0)$ in the units of a_\perp . Yellow represents the highest probability density region falling off to the least in the blue region shown in the vertical color bar.

	$g_2 = -1$		$g_2 = +1$	
σ	E_{sat}	Hilbert space \tilde{N}_c	E_{sat}	Hilbert space \tilde{N}_c
0.1	0.4238	139	1.2044	107
0.2	0.6008	37	1.2261	25
0.4	0.7333	13	1.2172	12
0.6	0.8079	6	1.1779	4
0.8	0.8583	3	1.1374	4
0.9	0.8773	3	1.1203	2

TABLE I: Active(critical) Hilbert space \tilde{N}_c for different interaction range σ for relative angular momentum $|m| = 0$ with interaction strength g_2 . Shows the variation of critical Hilbert space \tilde{N}_c with an increase in σ .

function and finite-range effects with the interaction strength g_2 in the subspace of relative angular momentum quantum number $|m| = 0, 1$. In the energy spectrum, the role of negative and positive interaction strength is extensively explored and observe that in single particle

	$ m = 0$		$ m = 1$	
g_2	E_{sat}	Hilbert space \tilde{N}_c	E_{sat}	Hilbert space \tilde{N}_c
-4	*	*	1.961	136
-3	*	*	1.975	72
-2	*	*	1.985	32
-1	0.425	81	1.993	04
1	1.206	33	2.006	06
2	1.309	25	2.010	26
3	1.361	39	2.015	28
4	1.396	52	2.018	47

TABLE II: Active Hilbert space \tilde{N}_c for different interaction range σ , relative angular momentum $|m| = 0, 1$ and interaction strength g_2 . For $|m| = 0$ the zero-point energy is $\hbar\omega$ and hence for $g_2 < -1$ becomes un-physical system.

angular momentum state $|m| = 0$, the energy spectrum $\epsilon_{n_r} = 2n_r + |m| + 1 + \underbrace{g_2 V(r)}_g - m\Omega/\omega_\perp$, we terminate our study at $g = -1$. Since the zero-point energy of a system of two spin-0 bosons in relative coordinates is $\hbar\omega$. Hence, for $g \leq -1\hbar\omega$, the system forms a bound state with energy < 0 . The strength $g \leq -1$ turns the system into a lump, which becomes independent of the quantum statistics and hence no further interaction will make any physical meaning, therefore we terminate our study at strength $g = -1$. In the rotating case, $|m| = 1$, has freedom in the sense that the strength $g = -(1 + |m| - m\Omega/\omega_\perp)$ can have different values of g_2 because there is no violation of quantum statistics. We further study the total ground state energy in terms of various components like trap potential $\langle PE \rangle$, interaction potential $\langle V_{\text{int}} \rangle$, kinetic $\langle KE \rangle$. We observe that the variation in the $\langle PE \rangle$, with respect to $\langle KE \rangle$ and $\langle V \rangle$ is very small. We also observe that E_0 increases with increase in interaction strength g_2 in both region $g_2 < 0$ and $g_2 > 0$, for a given $|m| = 0$ state, however in the case of relative angular momentum $|m| = 1$, the E_0 does not feel any kind of interaction strength because of the odd parity of relative angular momentum $|m|$. Further, we observe that for negative interaction strength $g_2 = -1$, the ground state energy $E_0(\tilde{N})$ follows the logarithmic convergence and hence the size of single-particle basis (as

a function of Hilbert space) increases infinitely. However for positive interaction strength $g_2 = +1, +2, +3, +4$, the ground state energy E_0 converges relatively for smaller values of single-particle basis as shown in Fig. 1. We observe that the choice of interaction strength, $g_2 = +1, +2, -1$ are the best choice for our finite-range study. As we know the Gaussian potential in Eq. 1, can be expanded within the finite number of single particle basis in contrast to the contact δ -function which takes infinite size in terms of single particle basis. The size of critical Hilbert space \widetilde{N}_c increases infinitely for $\sigma \rightarrow 0$ in case of relative angular momentum $|m| = 0$, for example: $\sigma = 0.001, 0.1, 0.3$ requires infinite basis size. For $\sigma \rightarrow 1$ requires a small basis size as shown in Fig.3.

Appendix A: Calculation of interaction matrix elements

In this appendix we outline the steps for calculation of the matrix elements used in the secular equation in the main text in Eq. 11) for that we consider a normalized single particle wavefunction $u_{n_r, m}(r_\perp \alpha_\perp, \phi)$ in relative coordinates and integrate it over $r dr d\phi$, where, r is spatial relative co-ordinate and ϕ is an azimuthal angle. The single particle interaction elements are being calculated in the following manner. The matrix elements are written in the following way.

$$I_{n'_r, |m'|; n, |m|}(\sigma) = \langle u_{n'_r, m'}(r_\perp \alpha_\perp, \phi) | V(r) | u_{n_r, m}(r_\perp \alpha_\perp, \phi) \rangle$$

and the single particle wavefunction,

$$u_{n_r, m}(r_\perp \alpha_\perp, \phi) = \sqrt{\frac{\alpha_\perp^2 n_r!}{\pi(n_r + |m|)!}} (r_\perp \alpha_\perp)^{|m|} e^{-\frac{1}{2} r_\perp^2 \alpha_\perp^2} \times e^{im\phi} L_{n_r}^{|m|}(r_\perp^2 \alpha_\perp^2) \quad (\text{A1})$$

where, $L_{n_r}^{|m|}(r_\perp^2 \alpha_\perp^2)$ is the associated Laguerre polynomials,

$$\begin{aligned} I_{n'_r, |m'|; n, |m|}(\sigma) &= \int_0^\infty \int_0^{2\pi} r_\perp dr_\perp d\phi \sqrt{\frac{\alpha_\perp^2 n_r!}{\pi(n_r + |m|)!}} \\ &\times (r_\perp \alpha_\perp)^{|m|} e^{-1/2 r_\perp^2 \alpha_\perp^2} e^{im\phi} \\ &\times L_{n_r}^{|m|}(r_\perp^2 \alpha_\perp^2) \times \frac{1}{2\pi\sigma^2} \exp\left(-\frac{r^2}{2\sigma^2}\right) \\ &\times \sqrt{\frac{\alpha_\perp^2 n'_r!}{\pi(n'_r + |m'|)!}} (r_\perp \alpha_\perp)^{|m'|} \\ &\times e^{-1/2 r_\perp^2 \alpha_\perp^2} e^{-im'\phi} L_{n'_r}^{|m'|}(r_\perp^2 \alpha_\perp^2) \end{aligned}$$

the integration is being carried out for the ϕ first, which gives delta function,

$$\begin{aligned}
I_{n_r, |m'|; n, |m|}(\sigma) &= \frac{1}{2\pi\sigma^2} \int r_\perp dr_\perp 2\pi\delta(m - m') \\
&\times \sqrt{\frac{\alpha_\perp^2 n_r!}{\pi(n_r + |m|)!}} (r_\perp \alpha_\perp)^{|m|} e^{-1/2r_\perp^2 \alpha_\perp^2} L_{n_r}^{|m|}(r_\perp^2 \alpha_\perp^2) \\
&\times \sqrt{\frac{\alpha_\perp^2 n_r'!}{\pi(n_r' + |m'|)!}} (r_\perp \alpha_\perp)^{|m'|} e^{-1/2r_\perp^2 \alpha_\perp^2} L_{n_r'}^{|m'|}(r_\perp^2 \alpha_\perp^2)
\end{aligned} \tag{A2}$$

we substitute $m = m'$ and get the following results

$$\begin{aligned}
I_{n_r, |m'|; n, |m|}(\sigma) &= \sqrt{\frac{n_r!}{\pi(n_r + |m|)!}} \sqrt{\frac{n_r'!}{\pi(n_r' + |m|)!}} \pi \frac{1}{2\pi\sigma^2} \\
&\times \int \underbrace{\alpha_\perp^2 2r_\perp dr_\perp}_{d(r_\perp^2 \alpha_\perp^2)} (r_\perp \alpha_\perp)^{2|m|} \exp(-r_\perp^2 \alpha_\perp^2 (1 + \frac{1}{2\alpha^2 \sigma^2})) \\
&\times L_{n_r'}^{|m|}(r_\perp^2 \alpha_\perp^2) L_{n_r}^{|m|}(r_\perp^2 \alpha_\perp^2)
\end{aligned} \tag{A3}$$

let $1 + \frac{1}{2\alpha^2 \sigma^2} = \Lambda$, another dimensionless quantity and

$$\begin{aligned}
I_{n_r, |m'|; n, |m|}(\sigma) &= \sqrt{\frac{n_r!}{\pi(n_r + |m|)!}} \sqrt{\frac{n_r'!}{\pi(n_r' + |m|)!}} \pi \frac{1}{2\pi\sigma^2} \\
&\int d(\alpha_\perp^2 r_\perp^2) (r_\perp \alpha_\perp)^{2|m|} \exp(-r_\perp^2 \alpha_\perp^2 \Lambda) L_{n_r'}^{|m|}(r_\perp^2 \alpha_\perp^2) L_{n_r}^{|m|}(r_\perp^2 \alpha_\perp^2)
\end{aligned} \tag{A4}$$

again defining $r_\perp^2 \alpha_\perp^2 \Lambda = \rho$ in the form of a new dimensionless parameter and substituting it in the above expression which further simplifies,

$$\begin{aligned}
I_{n_r, |m'|; n, |m|}(\sigma) &= \frac{1}{2\pi\sigma^2 \Lambda} \sqrt{\frac{n_r!}{(n_r + |m|)!} \frac{n_r'!}{(n_r' + |m|)!}} \\
&\times \int d\rho \left(\frac{\rho}{\Lambda}\right)^{|m|} \exp(-\rho) L_{n_r'}^{|m|}\left(\frac{\rho}{\Lambda}\right) L_{n_r}^{|m|}\left(\frac{\rho}{\Lambda}\right) \\
&= \frac{1}{2\pi\sigma^2 \Lambda^{1+|m|}} \sqrt{\frac{n_r!}{(n_r + |m|)!} \frac{n_r'!}{(n_r' + |m|)!}} \\
&\times \int d\rho \rho^{|m|} \exp(-\rho) L_{n_r'}^{|m|}\left(\frac{\rho}{\Lambda}\right) L_{n_r}^{|m|}\left(\frac{\rho}{\Lambda}\right)
\end{aligned}$$

using multiplication formula for the associated Laguerre polynomials in the above integral to make it solvable by removing $1/\Lambda$ term from it [30]

$$L_{n_r}^{[m]}(\Lambda x) = \sum_{i=0}^{n_r} \frac{\Lambda^i (|m|+1)_{n_r} (1-\Lambda)^{n_r-i}}{(|m|+1)_i (n_r-i)!} L_i^{[m]}(x)$$

writing the expression in Pochhammer symbols, $P(a)_n$, the integrand is now a function of a single variable ρ which can be easily solved,

$$\begin{aligned} I_{n_r, |m'|; n, |m|}(\sigma) &= \frac{1}{2\pi\sigma^2 \Lambda^{1+|m|}} \sqrt{\frac{n_r!}{(n_r+|m|)!} \frac{n_r'!}{(n_r'+|m|)!}} \\ &\times \sum_{i, i'=0}^{\min(n_r, n_{r'})} \frac{\Lambda^{-i-i'} (|m|+1)_{n_r} (1-\Lambda^{-1})^{n_r+n_{r'}-i-i'}}{(|m|+1)_i (n_r-i)!} \\ &\times \frac{(|m|+1)_{n_{r'}}}{(|m|+1)_{i'} (n_{r'}-i')!} \int_0^\infty d\rho \rho^{|m|} \exp(-\rho) L_i^{[m]}(\rho) L_{i'}^{[m]}(\rho) \end{aligned}$$

using the orthogonality condition for the associated Laguerre polynomials, the expression becomes,

$$\begin{aligned} I_{n_r, |m'|; n, |m|}(\sigma) &= \frac{1}{2\pi\sigma^2 \Lambda^{1+|m|}} \sqrt{\frac{n_r!}{(n_r+|m|)!} \frac{n_r'!}{(n_r'+|m|)!}} \\ &\times \left(\frac{\Lambda-1}{\Lambda}\right)^{n_r+n_{r'}} \sum_{i=0}^{\min(n_r, n_{r'})} \frac{(|m|+1)_{n_r}}{(|m|+1)_i (n_r-i)!} \\ &\times \frac{(|m|+1)_{n_{r'}}}{(|m|+1)_i (n_{r'}-i)!} \frac{(i+|m|)!}{i!} \left(\frac{1}{(\Lambda-1)^2}\right)^i \end{aligned}$$

writing the Pochhammer symbol in terms of factorials, $(a)_n = \frac{(a+n-1)!}{(a-1)!}$ we have the following results.

$$\begin{aligned} I_{n_r, n_{r'}, |m|}(\sigma) &= \frac{1}{2\pi\sigma^2 \Lambda^{1+|m|}} \sqrt{\frac{n_r!}{(n_r+|m|)!} \frac{n_r'!}{(n_r'+|m|)!}} \\ &\times \left(\frac{\Lambda-1}{\Lambda}\right)^{n_r+n_{r'}} \sum_{i=0}^{\min(n_r, n_{r'})} \binom{|m|+n_r}{|m|+i} \\ &\times \binom{|m|+n_{r'}}{|m|+i} \frac{(|m|+i)!}{i!} \left(\frac{1}{(\Lambda-1)^2}\right)^i. \end{aligned}$$

(A5)

These results will be useful in the further study of problems in the main text with the original parameters.

Appendix B: Calculation of $c_{n_r,m}$.

In this section we perform the calculation for the expansion co-efficient used at Eq. 1.8 in the main text, however, the approach is general and can be found in any standard quantum mechanics text. We simply solve the following Hamiltonian operator, A different approach is given in [31].

$$\hat{H} = \underbrace{\hat{H}_0 - \hat{\Omega} \cdot \hat{\mathbf{L}}}_{H_{\text{sp}}} + g_2 W$$

where the H_{sp} is single particle Hamiltonian, we write the wavefunction in the product form of expansion co-efficient and single particle wavefunction,

$$|\psi_{n_r,m}\rangle = \sum_{n_r,m} c_{n_r,m} u_{n_r,m} \quad (\text{B1})$$

as the eigenenergy and eigenstates of unperturbed Hamiltonian is known to be. $H_{\text{sp}}|u_{n_r,m}\rangle = \epsilon_{n_r,m}|\psi_{n_r,m}\rangle$,

$$\begin{aligned} (H_{sp} + g_2 W)|\psi\rangle &= E|\psi\rangle \\ (E - H_{sp})|\psi\rangle &= g_2 W|\psi\rangle \end{aligned}$$

on operating $|u_{n_r,m}\rangle$ from right we get the following form

$$(E - \epsilon_{n_r,m})\langle u_{n_r,m}|\psi\rangle = g_2 \langle u_{n_r,m}|W|\psi\rangle \quad (\text{B2})$$

from the above equation, we get the expansion coefficients,

$$c_{n_r,m} = \langle u_{n_r,m}|\psi\rangle = \frac{g_2 \langle u_{n_r,m}|W|\psi\rangle}{E - \epsilon_{n_r,m}} \quad (\text{B3})$$

till now no approximation has been used, unknown $|\psi\rangle$ in the above equation is dependent on the co-efficient. We can set $|\psi\rangle = |u_{0,m}\rangle$ and $|\psi\rangle = |u_{r',m}\rangle$ for the study of ground and excited states respectively in A.4. The ground state

$$c_{n_r,m} = -\frac{g_2 \langle u_{n_r,m}|W|u_{0,m}\rangle}{(\epsilon_{n_r,m} - E)} \quad (\text{B4})$$

and the most general form for studying the higher excited states,

$$c_{n_r,m} = -\frac{g_2 \langle u_{n_r,m}|W|u_{n_{r'},m}\rangle}{(\epsilon_{n_r,m} - E)}. \quad (\text{B5})$$

we can arrive at the exact and approximate solution in the main text.

Appendix C: Expectation of trap potential.

This expectation gives the matrix elements for the trapping potential of the harmonic oscillator, this calculation is based on the basic quantum mechanics technique and can be found in any standard textbook.

$$\begin{aligned}
\langle \alpha^2 r^2 \rangle = & \int_0^\infty \int_0^{2\pi} r_\perp dr_\perp d\phi \sqrt{\frac{\alpha_\perp^2 n_r!}{\pi(n_r + |m|)!}} \\
& \times (r_\perp \alpha_\perp)^{|m|} e^{-1/2 r_\perp^2 \alpha_\perp^2} e^{im\phi} \\
& \times L_{n_r}^{|m|}(r_\perp^2 \alpha_\perp^2) \times r^2 \alpha^2 \\
& \times \sqrt{\frac{\alpha_\perp^2 n_r'!}{\pi(n_r' + |m'|)!}} \\
& \times (r_\perp \alpha_\perp)^{|m'|} e^{-1/2 r_\perp^2 \alpha_\perp^2} e^{-im'\phi} \\
& \times L_{n_r'}^{|m'|}(r_\perp^2 \alpha_\perp^2)
\end{aligned}$$

first, we have integrated over the ϕ , and from there a factor of $2\pi\delta_{m,m'}$ simplifies the integration in the following way, similar steps as in the earlier calculations

$$\begin{aligned}
= & \sqrt{\frac{n_r'! n_r!}{(n_r + |m|)!(n_r' + |m|)!}} \int_0^\infty d(\alpha_\perp^2 r_\perp^2) (r_\perp^2 \alpha_\perp^2)^{|m|+1} \\
& \times e^{-r_\perp^2 \alpha_\perp^2} L_{n_r}^{|m|}(r_\perp^2 \alpha_\perp^2) L_{n_r'}^{|m|}(r_\perp^2 \alpha_\perp^2)
\end{aligned}$$

using orthogonality relation of associated Laguerre polynomials,

$$= \sqrt{\frac{n_r'!(n_r + |m|)!}{n_r!(n_r' + |m|)!}} (2n_r + |m| + 1) \quad (C1)$$

for $m = 0$ the above equation simplify to the simple form $2n_r + 1$.

-
- [1] B. Partoens, A. Matulis, and F. M. Peeters, Phys. Rev. B **59**, 1617 (1999).
 - [2] See, Proceedings of the International School of Physics “Enrico Fermi,” Course CXL, 1999, edited by M. Inguscio, S. Stringari, C. E. Wieman (IOS Press, Netherlands, 1999).
 - [3] Rajibul Islam, Ruicho Ma, Philipp M. Preiss, M. Eric Tai, Alexander Lukin, Matthew Rispoli, and Markus Greiner, Nature **528** 77-83 (2015).
 - [4] S. Inouye, M.R. Andrews, J. Stanger, H.J. Miesner, D.M. Stamper-Kurn and W. Ketterle, Nature (London) **392**, (1998) 151.

- [5] Rostislav A. Doganov, Shachar Klaiman, Ofir E. Alon, Alexej I. Streltsov and Lorenz S. Cederbaum, Phys. Rev A **87**, 033631 (2013).
- [6] Peter Jeszenszki. Ali. Alavi and Joachin Brand, Phys. Rev. A **99**, 033608 (2019).
- [7] A.D.Lange, K.Pilch, A. Pranter, F.Ferlaino, B. Engeser, H.-C. Nägerl, R. Grsimm and C. Chin, Phys. Rev. A **79**, 013622 (2009).
- [8] K. D. Sen, H. E. Montgomery Jr, Bowen Yu and Jacob Katriel, Eur. Phys J. D, **75**, 175, (2021).
- [9] T. Busch, B.-G. Englert, K. Rzażewski and Kazimierz Wilkens. Found. Physics,**549**, 498 (1998).
- [10] Thomas Busch, Berthold-Georg Englert, Kszimierz Rzazewski and Martin Wilkens, Found. of Phys, **28**, 550, (1998).
- [11] Luca Salasnich and Boris A. Malomed, Phys. Rev. A **79**, (2009), 053620.
- [12] F. Dalfovo, S. Giorgini, L. P. Pitaevskii and S. Strongari, Rev Mod. Phys. **71**, (1999), 463.
- [13] Mohd Imran and M A H Ahsan, J. Phys. B: At. Mol. Opt. Phys **53**,125303 (2020).
- [14] J. Christensson, C. Forssen, S. Aberg and S. M. Reimann, Phys. Rev A, **79**, 012707 (2009).
- [15] D. Blume, and Chris H. Greene, Phys. Rev. A **65**, 043613 (2002).
- [16] C.C Bradley, C.A Sackett, J.J. Tollett, and R.G. Hulet, Phys. Rev. Lett. **75**, 1687 (1995).
- [17] Thomas Busch, Berthold-Georg Englert, Kazimierz Rzażewski and Martin Wilkens. Foundations of Physics, **549**, 498 (1997).
- [18] Przemyslaw Koscik and Tomasz. Sowinsk. Scientific reports **8**,18505 (2018)
- [19] D. Blume, Rep. Prog. Phys. **75** (2012) 046401 (37pp)
- [20] Pere Mujal, Artur Polls and B Juliä-Díaz, Condens. Matter., **3** 9, (2018)
- [21] Shachar Klaiman, Nimrod Moiseyev and Lorenz S Cederbaum. Phys. Rev. A **73**, 013622 (2006).
- [22] M. A. H. Ahsan and N. Kumar, Phys. Rev. A **64**, 013608 (2001).
- [23] Anna Dawid, Maciej Lewenstein, and Michał Tomza, Phys. Rev A, **97**, 063618 (2018).
- [24] M.L. Boas, *Mathematical Methods in the Physical Sciences* (John Wiley and Sons, New York, 1983)
- [25] Mohd Imran and M.A.H. Ahsan, Communications in Theoretical Physics **65** 4, 473, (2016).
- [26] S. Inouye, M.R. Andrews, J. Stenger, H.J. Miesner, D.M. Stamper-Kurn, and W. Ketterle, Nature (London) **392**, 151 (1998)

- [27] C. J. Pethick and H. Smith, *Bose-Einstein condensate in dilute Bose Gases*, (Cambridge University Press, Cambridge, 2002).
- [28] Xia-Ji Liu, Hui Hu, Lee Chang and Shi-Qun Li, Phys. Rev A, **64**, 035601 (2001)
- [29] H. Saarikoski, S. Reimann, A. Harju, and M. Manninen, Rev. Mod. Phys. **82**, 2785 (2010).
- [30] D.D Tcheutia, M. Foupouagnigni, W. Koepf, P. Njionou Sadjang, The Ramanujan J. , (2016), 498.
- [31] Xia-Ji Liu, Hui Hu and Peter D. Drummond, Phys. Rev B, **82**, 054524 (2010).